Protoplasma (2010) 243:73–86
DOI 10.1007/s00709-010-0123-y

ORIGINAL ARTICLE

Physiological and morphological processes in the Alpine snow alga *Chloromonas nivalis* (Chlorophyceae) during cyst formation

Daniel Remias · Ulf Karsten · Cornelius Lütz · Thomas Leya

Received: 4 December 2009 / Accepted: 15 February 2010 / Published online: 14 March 2010
© Springer-Verlag 2010

Abstract Amongst a specialised group of psychrophilic microalgae that have adapted to thrive exclusively in summer snow fields, *Chloromonas nivalis* has been reported as a species causing green, orange or pink blooms in many alpine and polar regions worldwide. Nevertheless, the cytology, ecophysiology and taxonomy of this species are still unresolved. Intracellular processes during cyst formation, which is the dominant stage on snow fields, were examined with samples from the European Alps to better understand the cellular strategies of a green alga living in this harsh habitat. We show with two different methods, i.e. oxygen optode fluorometry and by chlorophyll fluorescence, that the cysts are photosynthetically highly active, although they do not divide, and that *Chloromonas nivalis* can cope with low as well as high light conditions. During cyst formation, the chloroplast is fragmented into several smaller parts, enlarging the surface to volume ratio. The pool of xanthophyll-cycle pigments is significantly enlarged, which is different from other snow algae. The cytoplasm is filled with lipid bodies containing astaxanthin, a secondary carotenoid that causes the typical orange colour. The cyst wall surface possesses characteristic elongate flanges, which are assembled extracellulary by accumulation of material in the periplasmatic interspace. Comparison of *Chloromonas nivalis* samples from different locations (Austrian Alps, Spitsbergen) by molecular methods indicates genetic variations due to spatial isolation, while a North American strain has no close relationship to the taxon.

Keywords Algal photosynthesis · Astaxanthin · Cyst ultrastructure · Taxonomy · UV protection

Abbreviations

LM	light microscopy
MAA	mycosporin-like amino acid
SEM	scanning electron microscopy
TEM	transmission electron microscopy
VAZ	violaxanthin, antheraxanthin and zeaxanthin

Electronic supplementary material The online version of this article (doi:10.1007/s00709-010-0123-y) contains supplementary material, which is available to authorized users.

D. Remias (✉) · C. Lütz
Institute of Botany, University of Innsbruck,
Sternwartestr. 15,
6020 Innsbruck, Austria
e-mail: Daniel.Remias@uibk.ac.at

U. Karsten
Institute of Biological Sciences-Applied Ecology,
University of Rostock,
Albert-Einstein-Str. 3,
18059 Rostock, Germany

T. Leya
Fraunhofer-IBMT,
Am Mühlenberg 13,
14476 Potsdam-Golm, Germany

Introduction

The green alga *Chloromonas nivalis* (Chodat) Hoham et Mullet comb. nov. belongs to a distinct group of specialised autotrophic microorganisms, which have adapted to thrive exclusively in the niche of long-lasting polar and alpine summer snowfields (Hoham and Duval 2001). In general, such algae have to tolerate extreme light, low temperature and poor nutritional conditions (Komárek and Nedbalová 2007). Mass accumulations cause striking colourations of the snow surface during the melting period due to the cellular pigments.

The well-known and frequently investigated species of this cold habitat is *Chlamydomonas* cf. *nivalis*, which causes the "Red Snow" phenomenon in many places of the world (Harris 2009; Kol 1968). In contrast, *Chloromonas nivalis* generates, depending on the content of secondary carotenoids, green-, brownish-orange- or pink-coloured snow (Hoham and Mullet 1977; Leya 2004; Nedbalová et al. 2008; own observations). This taxon is found less frequently in continental Europe, and only a few reports of occurrence exist (Bischoff 2008; Ettl 1968; Kol 1968; Lukavský 1993). In the province Tyrol, Kol (1970) observed only isolated scattered cells of *Chloromonas nivalis* in red snow dominated by *Chlamydomonas nivalis*. Although a general lack of physiological and cytological data of *Chloromonas nivalis* exists, few recent studies evaluated the photosynthetic performance of isolates from Czechia using chlorophyll fluorescence measurements (Stibal 2003) as well as the genetics and morphology of samples from Japanese mountains (Muramoto et al. 2008). Nonetheless, a broader survey of this taxon is necessary in order to understand its survival strategies in a harsh habitat like snow.

Most commonly, the snow surfaces are populated by immotile mature cysts. This cell stage in the life cycle of *Chloromonas nivalis* can be easily determined by light microscopy (LM) or scanning electron microscopy (SEM) due to the specific cell shape and secondary cell surface structures (undulated flanges). Though less striking in morphological differences to other Chlamydomonad species, field material of the motile, flagellated cells (which are restricted to conditions deeper in the snow, e.g. less irradiation) show a characteristic, slightly asymmetrical and spindle-like morphology as described by Ettl (1983). Moreover, these motile *Chloromonas nivalis* cells are found only for a short period of time in the field because they quickly cease any cellular divisions and start a rapid process of cyst formation into robust spores. This can be triggered by nitrogen depletion in snow (Hoham and Duval 2001). The spores have then to cope with different harsh environmental conditions.

The cells are at first typically located at the snow surface, followed by exposure to dryness and high temperatures on the rock ground after non-permanent snow has melted in late summer.

In the present study, all investigations were undertaken with freshly collected field samples from the Austrian Alps, where *Chloromonas nivalis* causes occasionally mono-specific blooms. Field material was used because snow algae are difficult to cultivate and the germination of mature cysts, to our knowledge, has never been successfully induced under controlled laboratory conditions.

The morphology was evaluated by means of LM, SEM and transmission electron microscopy (TEM). Photosynthesis was measured with two different techniques to evaluate the differences and individual advantages of (a) a Fluoro-Optode system (PreSens) and (b) a fast chlorophyll fluorimeter (PAM, Walz). Pigment analysis, alpha-tocopherol quantification and screening for UV-absorbing mycosporin-like amino acids (MAAs) as well as for water-soluble phenolics were performed by high performance liquid chromatography (HPLC). These substances and their qualitative and quantitative changes during cyst formation were examined because of their ecological functions as intracellular protectants, e.g. against high irradiation or because of their antioxidant properties (Bidigare et al. 1993; Karsten et al. 2009). A molecular analysis (18S rRNA) was undertaken to evaluate the taxonomic position of *Chloromonas nivalis* amongst other, similar Chlamydomonadaceaen species from cold habitats. Finally, abiotic field parameters such as solar irradiance, pH, conductivity and the nutrient availability in the snow were recorded too.

The overall aim of the work was to understand the principal cytological and physiological adaptation strategies of *Chloromonas nivalis*, depending on the specific stage within the life cycle, considering limiting environmental factors like low light (under snow), excessive light (on snow surface), temperatures in combination with water availability (freeze–thaw cycles) and low nutrients of the habitat. To our knowledge, this paper is the first report where physiological and morphological comparisons between vegetative cells (at the beginning of their transition) and mature cyst stages of a snow alga were undertaken.

Materials and methods

Sampling, snow measurements and microscopy

Snow fields, containing almost exclusively cells of *Chloromonas* cf. *nivalis* (Chodat) Hoham and Mullet were harvested at Kühtai, Tyrol, Austria, in the proximity of Gossenkölle Lake, 2,419 m, N47°13.751 E11°00.803. There, the alga causes local blooms at mountainsides each season between May and July, typically from surface to a depth of 10 to 15 cm. Collections took place in 2004, 2008 and 2009 (dates in Table 1). Prior to physiological or biochemical measurements, the snow was gently melted at 4°C to 5°C and approximately 50 to 100 μmol PAR (photosynthetic active irradiance) $m^{-2}s^{-1}$. The algae were kept in their own cold melt water.

Snow temperatures were logged with TidbiT v2 sensors (Onset Cooperation, USA), and irradiation was recorded with a PMA2100 system (Solar Light, USA) according to Remias et al. (2009). Electrical conductivity and pH of melt water samples were obtained with WTW Instruments (Cond

Table 1 Collection data of *Chloromonas nivalis* field samples from the Tyrolean Alps

Date or reference	Location, elevation	µS cm^{-1}	pH	Cell length	Cell width	Snow colour
19 Aug 2004, this work	Alps, 2,478 m	3.6	6.0	21.5±1.6	12.6±1.3	Orange/brown
10 Jul 2008, this work	Alps, 2,503 m	2.8	5.0	14.5±2.0	9.7±1.2	Yellow/brown
24 Jul 2008, this work	Alps, 2,503 m	4.9	4.6	19.3	12.4	Yellow/brown
03 Jun 2009, this work	Alps, 2,419 m	5.4	6.2	22.0±1.6	13.4±1.1	Orange/brown
01 Jul 2009, this work	Alps, 2,463 m	7.2	5.4	23.5±1.8	14.0±1.0	Pink
Hoham and Mullet 1977	Cascade Mts., 1,387 m	n/a	5.0–5.1	16–37	10–21	Green
Leya 2004	Spitsbergen, coastal	12–57	5.4	26–29	10–13	Orange
Lukavský 1993	Czechia, 1,090 m	n/a	5.4	20–21	11–13	Green

Snow parameters and average cell sizes are compared with three other studies

340i, Inolab pH; Weilheim, Germany). Nutrient concentrations of melt water were measured colourimetrically with Spectroquant kits (for PO_4-P, NH_4-N, NO_3-N and Fe; Merck, Germany), using a Lambda 800 spectrophotometer (Perkin Elmer, USA).

LM was performed with a Axiovert 200 M (Zeiss, Germany); photos were taken with a Zeiss Axiocam MRc5. Specimen cooling to 1°C during observation to prevent any temperature stress was accomplished with a temperature-controlled chamber according to Buchner et al. (2007). Cyst samples for SEM were dried at 50°C for 12 h and afterwards contrasted without forgoing dehydration and critical-point drying for direct analysis in a Phillips SEM XL20.

For TEM, 1.25% glutaraldehyde and 1% OsO_4 fixation in 10 mM cacodylate buffer, dehydration in ethanol and embedding in epoxide resin (Agar Scientific, UK) was done according to Remias et al. (2009). Samples were examined with a Zeiss Libra 120 TEM at 80 kV.

Molecular analysis

The 2004 field samples of *Chloromonas nivalis* were used for molecular analysis (sample P24/DR4). Sequences of the 18S rRNA gene used in this study were obtained either from clonal cultures of the Culture Collection of Cryophilic Algae (CCCryo) at the Fraunhofer-IBMT in Potsdam (see CCCryo strain number numbers in ESM Table 1) or the relative gene was cloned from respective field samples. Sequences are available from GenBank under the accession numbers stated in ESM Table 1. From all samples, genomic DNA was isolated using the DNeasy Plant Kit (Qiagen, Hilden, Germany). PCR was performed on whole genomic DNA using the forward primer NS1 (5′-GTAGTCATATGCTTGTCTC-3′) and the reverse Primer 18L (5′-CACCTACGGAAACCTTGTTAC GACTT-3′). PCR products were purified with the QIAquick PCR Purification Kit (Qiagen). The PCR product was sequenced directly using the forward primers 34F (5′-GTCTCAAAGATTAAGCCATGC-3′), E528F (5′-TGCCAGCAGCYGCGGTAATTCCAGC-3′) and 920F (5′-GAAACTTAAAKGAATTG-3′), 1422F (5′-CAGGTCTGTGATGCCCTTAG-3′) and the reverse primers 536R (5′-GWATTACCGCGGCKGCTG-3′), 895R (5′-AAATCCAAGAATTTCACCTC-3′) and 1263R (5′-GAACGGCCATGCACCACC-3′). For some samples, the PCR product had to be cloned in *Escherichia coli* using the pGem-T Easy Vector System (Promega GmbH, Mannheim, Germany). Competent cells of *E. coli* were obtained from the strain XL1-Blue MRFMRF' according to Hannahan (1983). All working kits were used respective to manufacturer's instructions. The cloned PCR product was sequenced with the primers stated above. The gene sequences obtained were assembled and aligned using the CLC Combined Workbench software (version 3.6.2, CLC bio, Aarhus, Denmark). The alignment was imported into the phylogenetic software PAUP* 4.0 (beta version 10, Sinauer Associates, Inc., Sunderland MA, USA). To choose the best-fit evolutional model for nucleotide substitution, the data were analysed using version 3.7 of the software Modeltest (Posada and Crandall 1998). Final data analysis, analyses of bootstrap values and phylogenetic tree building were performed with the PAUP software.

Chromatography, photosynthesis and chlorophyll fluorescence

The HPLC analysis was carried out with an Agilent ChemStation 1100, equipped with a diode-array- and fluorescence-detector. The method for chlorophylls, carotenoids and alpha-tocopherol is described in Remias and Lütz (2007) and the method for water-soluble phenolics screening in Remias et al. (2009). Analysis of MAAs was performed according to Karsten et al. (2009).

Two different methods were used for algal photosynthesis measurements (P/I-curves). First, a Fibox 3 oxygen optode (PreSens, Regensburg, Germany) in a setup with 3 ml thermostatic acrylic chamber DW1 (Hansatech Instruments,

UK) combined with a magnetic stirrer. Two milliliters of algal suspension was mixed with 1 ml of a 0.1 M HCO_3^- source before measurement. Light levels were calibrated with a Hansatech QRT1 PAR sensor and set with Hansatech A5 neutral filters. The maximum irradiation was limited to 1,394 µmol photons $m^{-2}s^{-1}$. The values of two respiratory dark phases (before and after the light cycle) were averaged. The O_2 production per time was based on the amount of total chlorophyll per sample.

Second, in vivo chlorophyll fluorescence parameters were measured on melted snow at approximately 0°C with a pulse-amplitude modulated fluorometer (PAM 2000, Heinz Walz GmbH, Effeltrich, Germany). The measuring principle was based on the technique of Schreiber et al. (1986); the nomenclature is according to Kromkap and Forster (2003). The algae were kept on the snow under dim light for 5 min before F_v/F_m was determined. Then, cells were exposed to 11 photon flux densities (PFDs) for 2 min each ranging from 11 up to 483 µmol photons $m^{-2}s^{-1}$. The actinic light was provided by a red LED (650 nm) of the fluorometer. After each light exposure, a saturating pulse was given to detect F_m and $\Delta F/F_m$'. The relative electron transport rate of PSII (rETR) was calculated:

$$\mathrm{rETR} = \Delta F/F_m^{'} \times \mathrm{PFD}$$

where $\Delta F/F_m$'=the effective PSII quantum efficiency and PFD=photon flux density. Photosynthesis–irradiance (PI) curves as rETR vs. PFD were calculated and fitted by the mathematical model according to Webb et al. (1974):

$$\mathrm{rETR} = \mathrm{rETR}_{\max} \times \left(1 - \exp^{\frac{-\alpha \cdot \mathrm{PFD}}{\mathrm{rETR}_{\max}}}\right)$$

where rETR=relative electron transport rate of PSII, $rETR_{max}$=maximum relative electron transport rate of PSII, α=initial slope alpha and PFD=photon flux density.

The light saturation point I_k and the light compensation point I_c of the PI curves were determined as the quotient of $rETR_{max}$ and the initial slope α (Henley 1993).

Results

Habitat conditions

The snow temperatures were short-term recorded at a depth of 10 cm (where colouration due to the presence of algae was still visible) to follow a daily course: during daytime, the temperature varied between 0.8°C and 0.1°C; however, during night, it remained constant slightly above 0.0°C for more than 9 h. Solar irradiation values were measured in June 2009, and PAR was recorded at noon with values between 2,062 µmol photons PAR $m^{-2}s^{-1}$ (maximum at full sun) and 836 µmol (minimum at scattered cloudy sky). At noon, UV-A showed a peak of 48.9 Wm^{-2} and UV-B of 306 mW m^{-2} (measured with erythema detector). Under scattered cloudy conditions, the radiation declined to a range from 30.2 to 5.2 Wm^{-2} and from 105 to 20.3 mW m^{-2}, respectively. The pH of the snow varied from 4.6 to 6.0, and the electrical conductivities of melt water were between 2.8 and 7.2 µS cm^{-1} (taken at five different times, Table 1). Melt water nutrients were measured on 24 July 2008. Free iron was 16.7, ammonium was 586 and nitrate 202 µg l^{-1}. Phosphate was below the detection limit (50 µg l^{-1}).

The harvested field samples contained almost exclusively *Chloromonas nivalis*. In the vicinity, red snow caused by *Chlamydomonas* cf. *nivalis* (which is the most frequent species in Tyrol; Remias et al. 2005) and green/orange snow caused by *Chloromonas brevispina* had also been found. Scattered cells of these two taxa were occasionally interspersed in the *Chloromonas nivalis* samples, however, in very low biomass portions <2%. In addition, less frequent snow algae like *Chloromonas rosae* var. *psychrophila* and large ovoid red species, resembling a four-flagellated *Chlainomonas* sp., were found. By molecular analysis, the latter turned out to be a yet unknown *Chloromonas* sp. (GU117574, GU117575) with close genetic relationship to *Chloromonas nivalis* (see snow algae taxonomy section).

Cell structure during cyst transformation

The "earliest" stages of *Chloromonas nivalis* concerning their life cycle were harvested on 10 July 2008. Motile flagellates (with typical attributes like stigma or pulsatile vacuoles) were not present anymore in the field sample; instead, the cells had lost their flagella and started to produce cytoplasmic lipid bodies, filled with secondary carotenoids (Fig. 1a). No cell divisions were observed, but many algae shed a smooth primary cell wall; field samples were full of such empty covers (Fig. 1b). The average cell sizes of all samples are summarised in Table 1 (and compared with those of other reports). Generally, *Chloromonas nivalis* grows significantly with the beginning of cyst formation because the size increases by about 30% within 14 days (compare lines 2 and 3 in Table 1, samples were collected at the same spot). Older cysts grew even further. This indicates that the cyst wall is expandable, albeit flanges are formed on their surface (Fig. 1b, e). A few cells showed a delayed development of these characteristic secondary wall structures during maturation despite a high abundance of lipid bodies and may resemble, as a consequence, a (probably artificial) snow algal genus reported as *Cryodactylon* (Kol 1968; Nedbalová et al., 2008). Mature cysts were harvested in 2004, July 2008 and 2009. In those cases, the surface colour of snow had shifted to orange, yellowish/brownish or to pink (Table 1). The secondary cell walls had fully developed ribs, and

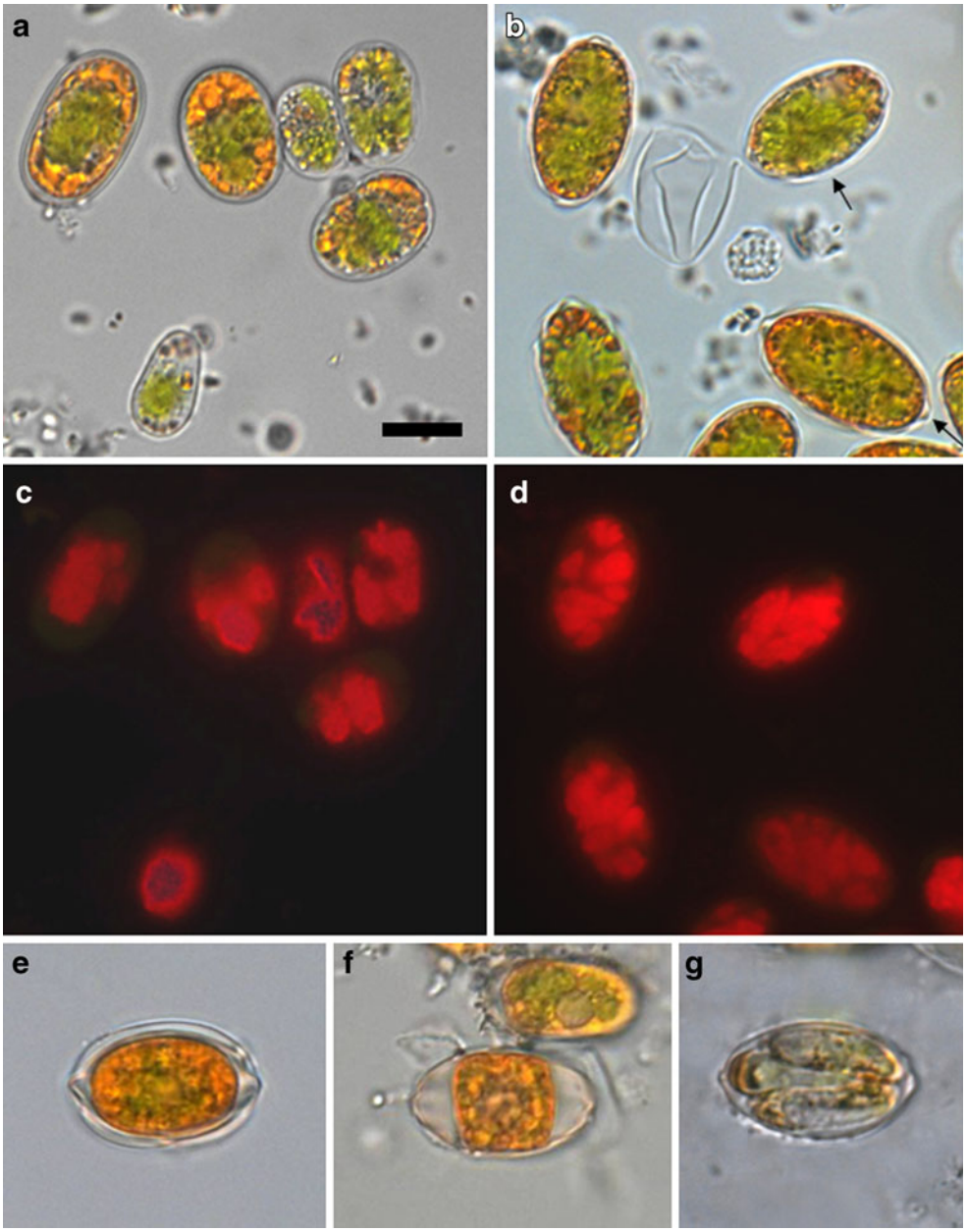

Fig. 1 Light micrographs of *Chloromonas nivalis*. **a** Young cysts with smooth cell walls. The smaller cells started the production of lipid bodies; **b** Cysts which possess already cell wall ribs (*arrows*). Note the empty cell wall cover in the *middle* which is shed before rib building; **c** and **d** Chlorophyll-autofluorescence images of **a** and **b**, showing a change in chloroplast structure during maturation from a compact form to fragmented smaller parts; **e** Mature cyst with ribbed cell wall and high amounts of cytoplasmic lipid bodies; **f** Old cyst, preparing for cell division by contracting the protoplast; **g** Final stage, before four smooth-walled, elongated daughter cells (one is not visible) will leave the old cyst by rupture. *Bar* 10 μm

sometimes inorganic snow detritus particles were adhered (Fig. 1f). The number of peripheral lipid carotenoid bodies visually increased, and they occupied a larger volume of the cytoplasm (Fig. 1e). The chloroplast (at least the visible green thylakoid fraction) had decreased in volume and was located in the middle of the cell. Fluorescence images revealed a structural change of the plastids: from an overall compact form in young cysts with some irregular lobes (Fig. 1c), they were reorganised into several smaller, rounded plate-like parts (Fig. 1d), thus increasing their effective surface. A pyrenoid was never visible. Cysts that were kept under laboratory conditions for several weeks started to contract the protoplast (Fig. 1f) and performed cell divisions, which resulted into four elongate, smooth-walled daughter cells (Fig. 1g). Unfortunately, no further cell divisions were observed to start a clonal culture, and we did not find this last stage directly in the snow; probably, in the field, it is formed only after a winter dormancy at the beginning of the next summer.

The ultrastructure of *Chloromonas nivalis* during cyst formation is presented in Fig. 2. The picture of a young cyst (Fig. 2a) shows the typical ovoid cell shape with a cell wall still without ribs and remnants of a shed outer wall. At its inner side, the periplasmatic interspace was occupied by large membrane-enclosed regions filled with unknown material, probably precursors for additional cell wall material. Further cytoplasmic structures are the nucleus, the lipid bodies (containing the secondary pigments),

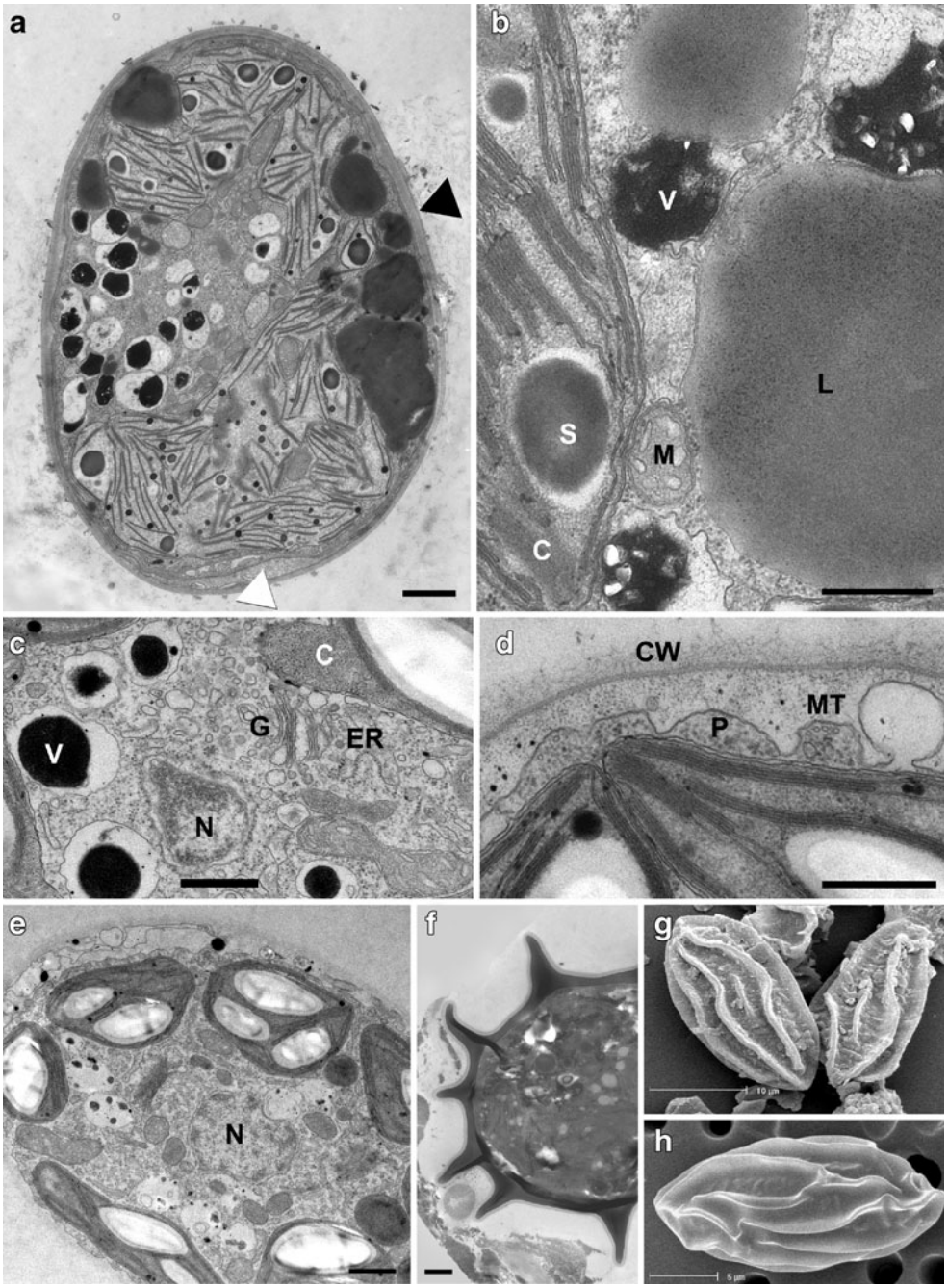

Fig. 2 TEM (**a**–**f**) and SEM (**g**, **h**) micrographs of *Chloromonas nivalis*. **a** Young cyst with one chloroplast. *White arrow*: material-filled interspace. *Black arrow*: trilaminar sheath still present at this spot, otherwise dissolved into loose flocky material; **b** Detail of a young cyst, chloroplast with starch (*S*), mitochondria (*M*), lipid bodies (*L*) and vacuoles (*V*) filled with crystalline material; **c** cytoplasm with Golgi vesicles (*G*) and rough ER (*ER*), showing high activity; **d** undulated plasmamembrane (*P*) with regularly arranged microtubules (*MT*) at the inner side. *CW*, cell wall; **e** Cyst with central nucleus (*N*), the chloroplast is divided into several smaller ones; **f** Section of a mature cyst, showing the bi-layered cell wall with ribs; **g** and **h** mature cysts, naturally covered with particles (**g**) or still uncovered (**h**). *C* chloroplast, *CW* cell wall, *L* lipid body, *M* mitochondria, *N* nucleus, *V* vacuole, *P* cytoplasm, *S* starch grain. *Bars* 1 μm (**a**, **e**, **f**), 0.5 μm (**b**–**d**)

mitochondria and several unidentified but noticeable organelles (vacuoles), which possess a compact electron-dense clump of material with embedded crystalline-like deposits (Fig. 2b). Well-developed Golgi bodies and a cytoplasm rich in vesicles and ribosomes indicate an active metabolism (Fig. 2c). Moreover, rough endoplasmic reticulum and a mitochondrion can be seen. Figure 2d points to the situation of a characteristically undulated plasmalemma, whose inner side frequently has "rows" of microtubules. The irregularly lobed, pyrenoid-free chloroplast contains scattered starch grains. In Fig. 2a, it is not yet divided into smaller parts, as seen in Fig. 2e in an older cyst. A section of mature cysts (Fig. 2f) shows a two-layered cell wall. SEM images of mature cysts reveal the taxonomically relevant composition of the undulated cell wall ribs. Not all of them completely reach from cell pole to cell pole; some end before or merge with other ones. Also, isolated short bands occur (Fig. 2g, h). The number of main ribs per cell section is usually between eight and nine.

Molecular grouping of snow algae

The phylogenetic maximum likelihood tree of various snow algal strains, based on 18S rRNA sequence data, is

presented in Fig. 3. The strains studied were assigned to different clades described in Pröschold et al. (2001), Hoham et al. (2002) and Leya (2004). Three sequences of *Chloromonas nivalis* from different geographic locations were included (Svalbard: CCCryo 005-99, Tyrolean Alps: P24/DR4, North America: UTEX B SNO66). All these strains belong to the "*Chloromonas*-Snow"-clade comprising all *Chloromonas* spp. from snow habitats. Nevertheless, several discrete clades are formed within this "*Chloromonas*-Snow"-clade indicating the polyphyly of *Chloromonas nivalis*. Since no living or preserved material is available as type strain, a definite assignment of either clade to this taxon is currently impossible. The overall results are summarised and evaluated in the discussion.

Pigment composition

Field material of *Chloromonas nivalis* was screened with two different methods for water-soluble, phenolic-like compounds and for MAAs. None of these substances were detected (data not shown). In contrast, this alga contains non-polar carotenoid pigments in high concentration. The relative amounts of primary (chloroplast-bound) and secondary (cytoplasmic lipid body bound) carotenoids are presented as ratios to chlorophyll a in Table 2. Also, chlorophyll b and alpha-tocopherol (vitamin E) were quantified using HPLC. The secondary colouration of *Chloromonas nivalis* is caused by the keto-carotenoid astaxanthin, and the majority of this pigment (69.9% to 100%, mean 91.2 %) is mono-esterified with a fatty acid, thus being more lipophilic as free astaxanthin. There has to be more than one type of associated fatty acid because at least two major peaks of astaxanthin-monoesters with different retention times but identical absorption spectra were detected. Only a very small amount of the astaxanthin occurs as the 13*Z cis*-isomer (maximum of 5.1% in sample from 01 July 2009), which can be identified by different absorption maxima closer to the UV-band and an additional absorption shoulder at 373 nm (HPLC online spectra). Other secondary carotenoids like canthaxanthin or echinenone were not detected. Young cysts (10 July 2008) contained less astaxanthin, thus appearing overall greener. The ratio of astaxanthin to chlorophyll a increased from 0.077 (10 July 2008) to 0.589 (19 August 2004); the latter value represents mature cysts. Notable changes in the commonly stable conditions of primary carotenoid ratios occurred with the xanthophyll-cycle components: the sum of violaxanthin, antheraxanthin and zeaxanthin (VAZ) increased from a ratio to chlorophyll a of 0.042 to 0.209, what is almost a five-fold increment of this photoprotective system. The xanthophyll-cycle deepoxidation state, expressed as (A+Z)/(V+A+Z), varied between 0.14 and 0.50. Moreover, mature cysts (19 August 2004) showed less chlorophyll b.

Photosynthesis

The light-dependent photosynthesis rates were obtained with two technically different methods, namely relative electron transport rate of photosystem II with a fluorometer (Fig. 4) and oxygen production with an optode (Fig. 5).

The relative electron transport rate as function of the photon fluence rate (PI-curve) was recorded and the data points fitted using the model of Webb et al. (1974). *Chloromonas nivalis* exhibited an α-value of 0.222, a relative ETR_{max} of 23.4 and an I_k value of 106 µmol photons $m^{-2}s^{-1}$ (Fig. 4), and no indication of photoinhibition up to the maximum photon fluence rate applied (483 µmol photons $m^{-2}s^{-1}$).

The data on oxygen consumption in the dark (respiration) and on oxygen evolution in the light between 54 and 1,394 µmol photons $m^{-2}s^{-1}$ were also fitted using the model of Webb et al. (1974). From the resulting photosynthesis–irradiance curve, a respiration rate of 25.2 µmol O_2 mg^{-1} Chl. *a* h^{-1}, a P_{max} of 191.8 µmol O_2 mg^{-1} Chl. *a* h^{-1}, an α-value of 1.69, an I_k value of 127.9 µmol photons $m^{-2}s^{-1}$ and an I_c value of 14.9 µmol photons $m^{-2}s^{-1}$ were calculated (Fig. 5). Similar to the PAM approach, no indication of photoinhibition up to the maximum photon fluence rate applied could be determined.

Discussion

Taxonomy of snow algae

The fusiform cysts of *Chloromonas nivalis*, with their characteristically ornamented cell wall surface with undulated flanges were initially believed to be a species of the immotile genus *Scotiella* (Kol 1968). Members of this genus are characterised by daughter cells having the same ribbed morphology when released from the mother cyst. Thus, *Chloromonas nivalis* was described as *Scotiella nivalis*, and Kol (1968) summarised reports of occurrence at many alpine and polar locations all over the world. This wrong diagnosis, however, was caused by the fact that the life cycle of this taxon was unknown for decades, especially concerning the short-lived vegetative cells (motile flagellates that lack any wall ornamentation) that were not observed yet, or such swarmers were not recognised as precursors of cysts in the field samples (a problem relevant to other snow algae, too). It was the merit of Hoham and Mullet (1977), who were the first to describe that cell size and morphology of this microalga change dramatically depending on the stage in the life cycle. Consequently, they transferred *S. nivalis* to *Chloromonas nivalis* (Hoham and Mullet 1978). *Scotiella* turned out to be an artificial genus, and those species that

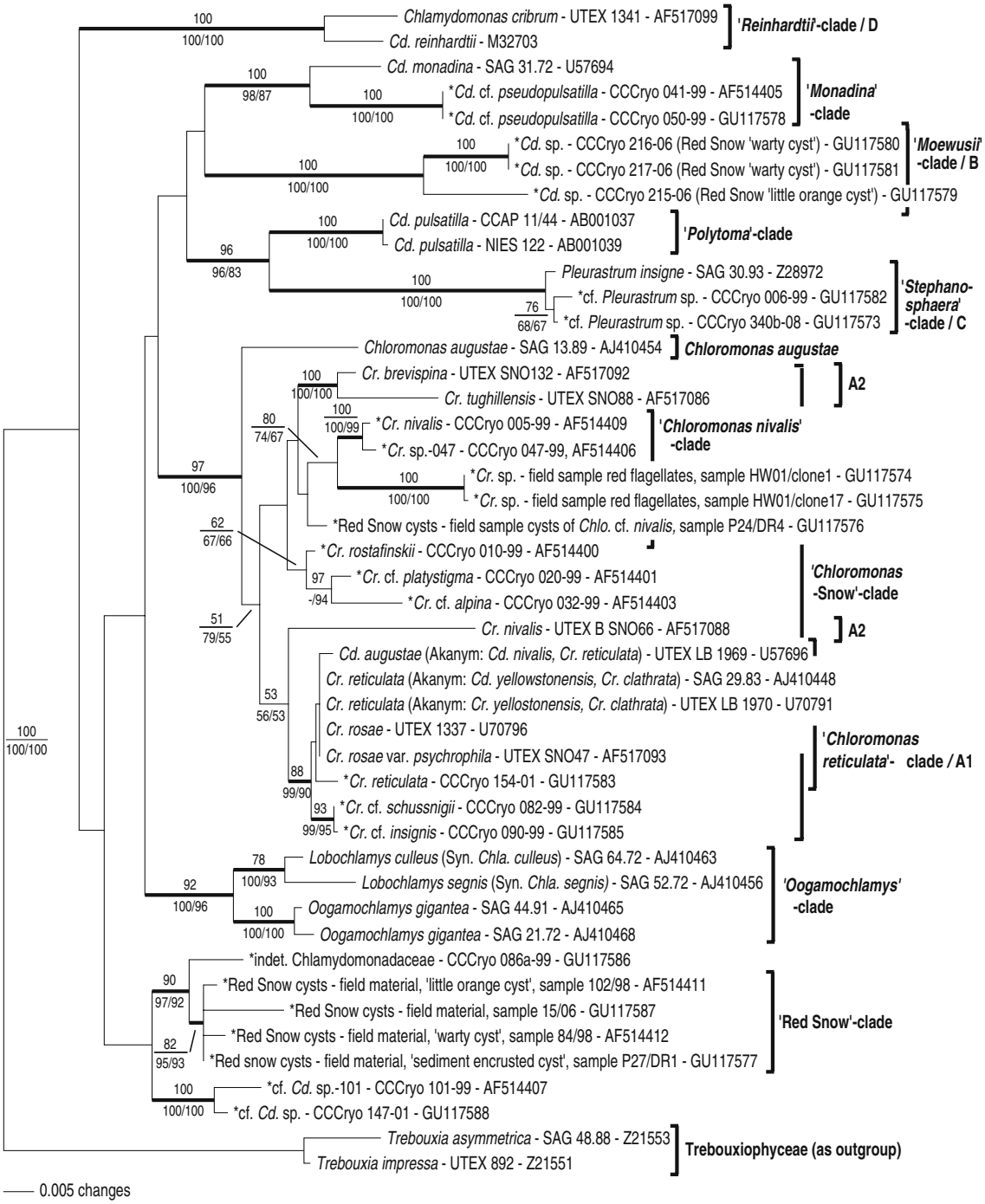

Fig. 3 Phylogenetic analysis of Arctic, Antarctic and European snow algal strains within the Chlamydomonadaceae based on nuclear-encoded 18S rDNA sequence comparisons (1,537 bp long; 94 variable and 269 parsimony-informative sites). Two Trebouxiophyceae were used as an outgroup. This maximum likelihood tree resulted from an analysis using the model of Tamura and Nei (1993) with proportions of invariable sites I=0.5574 and an estimated gamma shape G=0.6227. Bootstrap values at the branches were determined for maximum likelihood (*top*), minimum evolution distance (*bottom left*) and maximum parsimony (*bottom right*). *Thick lines* indicate branches with bootstrap values ≥75% under all three models. *Brackets* and clade assignments were stated according to Pröschold et al. 2001, Leya 2004 and Hoham et al. 2002. *Cd Chlamydomonas*, *Cr Chloromonas*, *asterisk*: prefix=sequences from this work

produce true "autospores" (meaning that daughter cells have the same cell wall morphology as the mother cell) were transferred into *Scotiellopsis* or *Coelastrella*, which, however, are not associated with snow habitats (Hanagata, 1998; Tschaikner et al. 2007). Further putative *Scotiella* species reported from snow, like *Scotiella polyptera* from Antarctica, were also revealed to be the spores of flagellated *Chloromonas*-like algae (Ling and Seppelt

Table 2 Pigment ratios (weight to weight) of different *Chloromonas nivalis* cyst maturation stages to chlorophyll a (=1)

	Neo	Lut	VAZ	EPS	β-Car	As	Chl b	α-toc
10 July 08 young (surface)	0.036	0.112	0.042	0.50	0.008	0.077	0.465	0.001
10 July 08 young (mixed)	0.031	0.129	0.037	0.41	0.012	0.129	0.405	0.001
03 June 09, mid-mature	0.045	0.158	0.103	0.14	0.019	0.474	0.499	0.004
01 July 09, mature	0.060	0.197	0.183	0.17	0.004	0.411	0.463	0.007
19 August 04, mature	0.047	0.188	0.209	0.27	0.008	0.589	0.349	0.005

Older cells contain more astaxanthin; moreover, the pool of xanthophyll-cycle pigments increases. The first two lines are from the same spot, but either surface or surface and depth harvest. *Neo* neoxanthin, *Lut* lutein, *VAZ* violaxanthin, antheraxanthin and zeaxanthin, *EPS* epoxidation state (AZ/VAZ), *β-Car* beta-carotene, *As* astaxanthin (free, all isomers and esters pooled), *Chl b* chlorophyll b, *α-toc* alpha-tocopherol

1998). Another example is *Scotiella cryophila* as an asexual resting spore of *C. rosae* var. *psychrophila* (Hoham et al. 2002). The main reason for earlier taxonomic misunderstandings was not only that flagellated cells are very short-lived in the field (and also overlooked when these stages were still hidden below a white snow surface in early summer), but also the fact that planozygotes with four flagella, a transient product of two fused biflagellate cells, were misinterpreted as a separate genus, e.g. like the most probably invalid species *Carteria nivalis*.

The cysts of *Chloromonas nivalis* described in the present study differ slightly in morphology from those from other regions. American samples of Hoham and Mullet (1977) have usually six to eight flanges in cross-section (in contrast to eight to nine in this work), and the cells are larger. Leya (2004) described populations from Arctic Spitsbergen with regularly undulated, continuous flanges without fusing/diverting ribs (the latter are typical for cells from the Alps). Also Müller et al. (1998) presented a cyst from snow collected in Spitsbergen with not all of the ribs reaching completely from pole to pole. Holzinger and Lütz (2006) used low-vacuum environmental scanning electron microscope for imaging *Chloromonas nivalis* from a snow field 23 km southeast from the location studied in this work and found similar results. SEM images of Japanese samples by Muramoto et al. (2008) indicated a somehow different structure of flanges which are stronger and more regular than those in this study, and they found two different morphotypes with straight or undulated ribs. Overall, the data of all these studies are not sufficient to clarify whether we are confronted with morphological variabilities extending over different populations or if these differences indicate indeed distinct taxa.

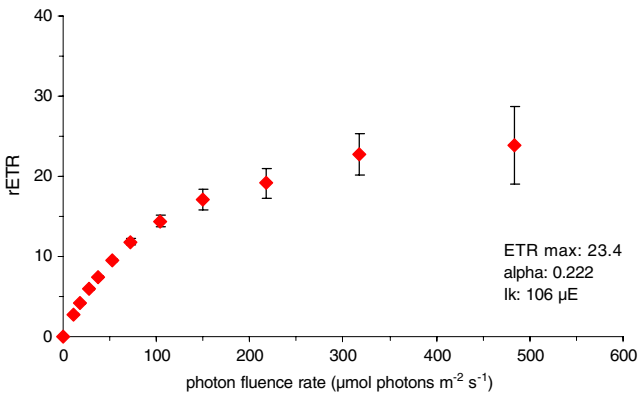

Fig. 4 The effect of increasing photon fluence rates on the relative electron transport rate (rETR) in *Chloromonas nivalis*. Each *symbol* represents the mean value of three replicate measurements (±SD). The data points were fitted with the photosynthesis model of Webb et al. (1974)

Considering the molecular data presented, it is clear that all populations earlier described as *Chloromonas nivalis*, sampled from different alpine and polar places worldwide, cannot be regarded as one identical species anymore. According to Kol (1968), who pointed out that *Chlamydomonas nivalis* has to be regarded as a collective taxon, this phylogenetic analysis and comparisons with earlier publications using either the 18S, the *rbc*L gene or both in combination (Hoham et al. 2002; Muramoto et al. 2008), reveal the same for *Chloromonas nivalis*. At least these two taxa, *Chlamydomonas nivalis* and *Chloromonas nivalis*, within the snow algae are polyphyletic. Consequently, the number of genetically different snow algal species worldwide with cysts resembling the "*Scotiella*"-type and thus, the species richness in these cold habitats is higher than expected, and the concept of a single cosmopolitan taxon has to be rejected.

Phylogenetically, the three sequences of *Chloromonas nivalis* obtained from either clonal cultures or cloned from field material occur at different positions within the "*Chloromonas*-Snow"-clade (Fig. 3). Hoham et al. (2002) associated their strain UTEX B SNO66 (=CU 563D) with this taxon based on a green culture sampled from Mount Lemon (Arizona, USA). Their sequence occurs at a basal position close to other *Chloromonas* spp. isolated from snow ("*Chloromonas reticulata*"-clade/A1 in Fig. 3). In either of their phylogenetic analyses based on 18S and *rbc*L sequences, analysed separately and combined, this strain occurs in their clade A2 together with *C. brevispina* (UTEX

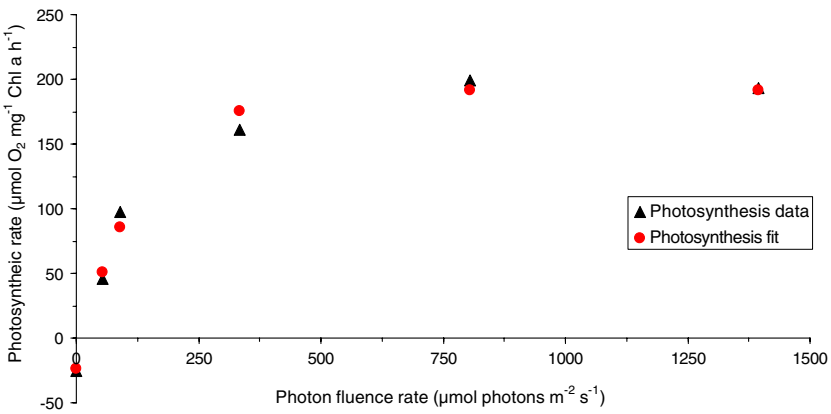

Fig. 5 Oxygen production and dark-respiration of *Chloromonas nivalis* at different light levels, measured by PreSens optode

SNO132), *Chloromonas tughillensis* (UTEX SNO88), *Chloromonas pichinchae* (UTEX SNO33) and two strains of *Chloromonas chenangoensis* (UTEX SNO147 and B SNO148; Hoham et al. 2002, 2006). In our phylogeny, this clade A2 is broadened by a number of sequences from different *Chloromonas* strains from snow habitats in Spitsbergen and the European Alps ("*Chloromonas nivalis*"-clade and the three other *Chloromonas* spp. below) cultured at the CCCryo. The low bootstrap values (<60%) for the branch above *Chloromonas nivalis* (UTEX SNO66) points to a weak robustness in our analysis. Muramoto et al. (2008) also analysed the phylogenetic position of three *Chloromonas nivalis* strains on the basis of *rbc*L data. One of their strains (Gassan-NIV2) appears close to *C. tughillensis* and *C. brevispina*, whilst the other (Gassan-NIV1) groups together with the UTEX SNO66 strain. Again, all three strains occur in the A2 clade mentioned above; however, again, low bootstrap values (<50 %) indicate the poor robustness of these phylogenetic relationships.

The second strain of *Chloromonas nivalis* analysed in this work is a clonal green culture from Spitsbergen (CCCryo 005-99). Whilst its natural morphology in field samples resembles much the description in Hoham and Mullet (1977), culture material soon loses typical features like, e.g. the tapered basal end of the cells. It groups together with the CCCryo strain 047-99 which again shows a slightly different morphology compared with CCCryo 005-99 (up to 32 daughter cells and a hardly tapered basal cell end), but probably can be considered as a variety of *Chloromonas nivalis*. Together with two clonal sequences from red-coloured field material (sample HW01), which was initially identified as a *Chlainomonas* sp. by light microscopy, and a clonal sequence of the spindle-like cyst material typical for *Chloromonas nivalis* (sample P24/DR4 from the Tyrolean Alps), these sequences form the "*Chloromonas nivalis*"-clade (Fig. 3). Whether the two sequences of sample HW01 really represent the genus *Chlainomonas* remains unclear. In this context, Novis et al. (2008) analysed the *rbc*L phylogeny of several *Chlainomonas* spp. and could establish separate clades [clades 1, 2 and 3 in Novis et al. (2008)] neighbouring clade A2 in Hoham et al. (2002). This basically corresponds to our analysis where the HW01 sequences occur in the "*Chloromonas nivalis*"-clade between the split clade A2 (Fig. 3). Novis et al. (2008) speculate whether the *Chlainomonas* sequences represent a lineage within the *Chloromonas* spp. arisen from the fusion of two ancestral biflagellated cells or whether they represent diploid forms of the same. Whether the genus *Chlainomonas* will remain valid needs further investigation.

Unfortunately, no *rbc*L sequence data for the CCCryo strains were available, and thus, no multi-gene analysis was possible for a direct comparison with the other publications stated above. However, with either phylogenetic analysis the overall picture remains the same. Only, in our phylogeny, the clade A2 is broadened by a number of *Chloromonas* spp. from snow in Spitsbergen (CCCryo strains) of which the 18S sequence data have not been included in other publications yet.

In summary, *Chloromonas nivalis* to date remains a cryptic species, in their cyst stage as well as when actively growing as green cell stages. The 18S and/or *rbc*L sequence data analyses reveal its polyphyletic evolution. A multi-gene approach (along with ITS 1/2) of all strains and cyst material available might finally elucidate its taxonomy.

The phylogenetic tree (Fig. 3) also includes other snow algal strains from the CCCryo analysed for the first time. It demonstrates well the general polyphyly of snow algae. As the Chlamydomonadaceae with its two major genera *Chlamydomonas* and *Chloromonas* are still undergoing major revisions (e.g. Pröschold et al. 2001), the taxonomic affiliation to either genus in Fig. 3 and ESM Table 1 is currently still tentative. According to the clade classification in Pröschold et al. (2001), various *Chlamydomonas*-like isolates from snow can be associated with the "*Monadina*"-(CCCryo strains 041-99, 050-99) or the "*Stephanosphaera*"-clade (CCCryo strains 006-99, 340b-08), or currently remain

unaffiliated (CCCryo strains 086a-99, 101-99, 147-01) but are closely related to snow algae forming the "Red Snow"-clade (Leya 2004). The latter clade comprises solely so far uncultured species of which sequences were obtained from red-coloured cysts from field samples. Such carotenoid-rich cysts often inhabit several square metres, forming the well-known phenomenon termed red snow or blood snow. Sequences in the *Chlamydomonas* "*moewusii*"-clade (CCCryo strains 215-06, 216-06, 217-06) were obtained from clonal cultures from cells that germinated from red snow collected at Spitsbergen ("warty cyst" and "little orange cyst"). Whether these sequences from the green (actively dividing) cell stages actually represent the respective red snow species still remains unconfirmed, as they are not homologous to those sequences determined for red-coloured resting stages ("warty cyst" and "little orange cyst") in the "Red Snow"-clade.

These data clearly point to an overall problem with resting stages from red snow, i.e. LM observations: The morphology of cells cannot elucidate differences between species. Furthermore, the red cysts do not germinate under laboratory conditions to form viable progeny.

Cell ultrastructure, pigment composition and ecology

The formation of cysts with thick, structured cell walls has the physiological advantage to reduce desiccation, penetration of harmful irradiance (UV) and grazing by animals and helps the cells to adhere to substrates after snowmelt (Hoham and Duval 2001; Holzinger and Lütz 2006). Such cysts may be necessary for successful airborne long-distance dispersal, as shown by Marshall and Chalmers (1997) for snow algae in Antarctica and by Bischoff (2008) for Switzerland. The process of rib formation is not yet fully understood, but it could be shown in the present study by TEM that young cysts accumulate large amounts of amorphous, putative cell wall material at the periphery of the cell and that it is enclosed by membranes which are likely exported through exocytosis into the periplasmatic space for assembling a new cell wall containing the flanges. Probably, rows of distinctly arranged microtubules next to the inner side of the plasmalemma play a role in controlling how and where the material is exported. Hepler and Newcomb (1964) found these regularly, parallel-orientated microtubuli in higher plants during secondary cell wall formation. Algal cysts are not exclusive to snow algae; nonetheless, only a few studies of their formation within the Chlamydomonadaceae exist. Brown et al. (1968) were the first who have indicated by TEM how secondary walls are formed, and the zygotes of *C. moewusii* have the same bi-layered type of wall like *Chloromonas nivalis* shown in Fig. 2e. Cavalier-Smith (1976) followed the zygospore formation in *Chlamydomonas reinhardii* and demonstrated that this process is accompanied by a general reduction of organelles like the chloroplast or the Golgi bodies; however, the multi-layered cell wall of this species is different to *Chloromonas nivalis*. Hoham and Blinn (1979) found the same bi-layered cyst wall at the snow alga *C. brevispina*, like in this study. Several studies investigated cyst walls of *Haematococcus pluvialis*, and Hagen et al. (2002) found similar results, like in this work, concerning a fast abandoned primary wall, a transient trilaminar sheath (=tripartite crystalline layer) with a thick secondary wall. These authors observed periplasmatic interspaces, filled with putative cell wall precursors, and the plasmamembrane was undulated in these regions as well.

A highly abundant secondary cytoplasmic pigmentation is a typical feature of most snow and ice algal species, and a photoprotective and ROS quenching function is evident (Bidigare et al. 1993). Besides, lipophilic pigments (in combination with lipids) go along with a lower water content of the cells and thus emend an avoidance of intracellular freezing at subzero temperatures. In addition, the content of lipophilic alpha-tocopherol generally increases during cyst maturation (Table 2). The presented TEM images illustrate that a large part of the cytoplasmic volume is occupied by lipid bodies but also by several specialised vacuoles, which are filled with unknown crystalline-like material.

In *Chloromonas nivalis*, astaxanthin in a mono-esterified form is the abundant secondary carotenoid causing the orange colour of the cytoplasmic lipid bodies. The same pigment induces the dark red colouration of the snow alga *Chlamydomonas* cf. *nivalis*, and the more intensive colour of that species is simply caused by the higher concentration of this secondary carotenoid (Bidigare et al. 1993; Müller et al. 1998; Remias et al. 2005). The Tyrolean samples of *Chlamydomonas nivalis* contain about 30% of their astaxanthin as 13*Z cis*-isomer, which has the benefit of an additional UV-A-absorption (Remias and Lütz 2007; general overview on carotenoid isomers in Liaaen-Jensen and Lutnæs 2008). Since *Chloromonas nivalis* from the Austrian Alps contains this *cis*-derivate only in much lower amounts (about 5%), and taken together with an overall lower astaxanthin level (approximately maximal ratio 0.6), this species may be less tolerant to high light stress than the cysts of "classical" red snow (which have ratios >8). In fact, red snow caused by *Chlamydomonas nivalis* can be found in highest elevations and most exposed sites, while we never found any populations of *Chloromonas nivalis* at extreme places like glacier surfaces or steep slopes. Consequently, the European *Chloromonas nivalis* may be a species adapted to lower mountain sites (e.g. in the Alps between 1,900 and 2,500 m above sea level; own observations) with less harsh abiotic conditions, which is consistent with reports of occurrence in several lower mountain ranges of Czechia (Lukavský 1993; Nedbalová

et al. 2008; Stibal 2003) or Bulgaria (Lukavský et al. 2009). Besides, the maximum field PAR-level of 2,062 µmol photons $m^{-2}s^{-1}$ measured in the present study was similar to reports from the Giant Mountains in Czechia (2,500 µmol photons $m^{-2}s^{-1}$, Nedbalová et al. 2008).

Concerning the pH of the snow, we did not find any trend of which values are preferred; they are generally slightly acidic as reported also by other authors (Table 1). The electrical conductivities of the Tyrolean snow water were always low, similar to pure water; only Leya (2004) had much higher levels in Spitsbergen, which may derive from nitrification due to the proximity of the sea and the presence of bird colonies.

Although the xanthophyll cycle of green algae is regarded as less effective as compared with higher plants concerning its contribution to non-photochemical-quenching (Masojídek et al. 2004), *Chloromonas nivalis* showed a notable trend of enhancing its VAZ pool about five-fold during cyst maturation. The relative quantity of these primary carotenoids, VAZ, to chlorophyll a and b changed from 0.026 (10 July 2008) to 0.154 (19August 2008). Other species that also produce secondary carotenoids in high abundances showed lower ratios like 0.078 (*H. pluvialis*) or 0.117 (*Chlorococcum* sp.) in the previous reference. Also, in a pigment productivity study of microalgae by Leya et al. (2009), it was reported that *Chloromonas nivalis* from Spitsbergen (strain CCCryo 005-99), like the alpine field samples of this study, have a large VAZ pool which is enlarged during maturation (ratio 0.07 in green and 0.249 in red samples). In this aspect, *Chloromonas nivalis* differs also from the species causing red snow (*Chlamydomonas* cf. *nivalis*) because the latter have only very low ratios of violaxanthin (e.g. 0.03 in Remias et al. 2005) and never showed any deepoxidation. Consequently, it can be assumed that *Chloromonas nivalis* may partly compensate light stress, which could reach the chloroplast more easily due to a lower amount of "shading" from secondary carotenoids in lipid globules, with an enlarged xanthophyll cycle.

The absence of MAAs in cysts of *Chloromonas nivalis* is not surprising, as these UV-sunscreen compounds have been found so far only in distinct groups of green algae such as various members of the Trebouxiophyceae (Karsten et al. 2005), but not in chloromonads yet. In the latter group, the astaxanthin can partly compensate the need of UV protection (Remias and Lütz 2007). The situation for UV-absorbing phenolics remains more unclear. While no water-soluble phenolics were found in this study for *Chloromonas nivalis* by HPLC, Li et al. (2007) measured phenolics semiquantitatively with a colourimetric assay for *Chlamydomonas nivalis* (the geographical origin of their red snow alga is not indicated) in polar and apolar solvent fractions. These phenolics had only a low antioxidative capacity comparing to those of higher plants. Duval et al. (2000) also used a colourimetric assay for the detection of phenolics in cysts of *Chlamydomonas nivalis*. However, both photometric methods cannot elucidate the structure of the actual molecules which reacted in their biotests. Phenolics and their ecological role in seaweeds or higher plants are well known (Leslie 2009), but their occurrence and abundance in freshwater microalgae still needs further work.

Photosynthesis

Direct comparisons between PAM derived photosynthetic electron transport rate (ETR) and oxygen evolution rate are generally difficult because there are fundamental differences in the nature of both methodological approaches. While the PAM is based on measurement of the in vivo variable chlorophyll a fluorescence of photosystem II, i.e. the photochemical efficiency, the oxygen method detects light-driven oxygen release from water molecules at the water-splitting side of photosystem II. There are many reports in the literature to evaluate the relationship between PAM fluorescence and oxygen evolution in micro- and macroalgae, and both linear and non-linear relationships have been described (Hancke et al. 2008, and references therein). In the present study, quite similar photosynthesis/irradiance curves were gained with both methodological approaches (Figs. 4 and 5). While applying the PAM led to an I_k value of 106 µmol photons $m^{-2}s^{-1}$, the optode system resulted in an I_k value of 127.9 µmol photons $m^{-2}s^{-1}$. Both values, together, with the low light compensation point (I_c) of 14.9 µmol photons $m^{-2}s^{-1}$, indicate moderate light requirements for photosynthesis in *Chloromonas nivalis*. These light curve data point to an alga that can be photophysiologically characterised as between low- and high-light adapted. Still, both the PAM and the optode system clearly indicate that no photoinhibition could be observed in *Chloromonas nivalis*, what can be seen as advantage at occasional high-light situations. In contrast, the snow alga *Chlamydomonas nivalis* is considered as truly high-light adapted (Gorton et al. 2001, Remias et al. 2005, Stibal et al. 2007).

From an ecophysiological point of view, the accumulation of secondary carotenoids has also the advantage to be a nitrogen-free "sink" for photosynthetic energy, which is sufficiently provided since these cysts do not represent a metabolic "resting stage" due to their high photosynthetic activity at irradiation conditions common on snow. Recently, also the cysts of another similar snow algal species, *C. brevispina*, were demonstrated to be photosynthetically active (Kvíderova et al. 2005). By using chlorophyll fluorescence, they measured an α-value of 0.29, a relative ETR_{max} of 73.4 and an I_k value of 250 µmol photons $m^{-2}s^{-1}$, suggesting a better high-light acclimation than *Chloromonas nivalis*.

As a consequence, snow algal cysts are active and can channel their photochemical energy into storage deposits like starch, soluble sugars, lipids and secondary carotenoids, despite their nitrogen-poor habitat. In this regard, Hoham and Mullet (1977) measured 40 μg l^{-1} NH_3-N and 2 μg l^{-1} NO_2-N in snow from North America, which is even only about one tenth and one hundredth of our results, respectively. Řezanka et al. (2008) found a so far unknown class of astaxanthin–diglucoside–diesters in red snow from Bulgaria, which combines three different kinds of storage metabolites, namely the secondary carotenoid, two sugars and two fatty acids. This compound amounted to 0.93% of the algal fresh weight.

Since cysts of *Chloromonas nivalis* do not divide for the rest of the season albeit being physiologically active, the energy provided by photosynthesis can be invested into significant growth during maturation (as shown in Table 1) and for later cell cleavages. The formation of daughter cells had only been observed in old field samples kept under culture conditions for several weeks at 4°C, but never in situ. Most likely, these cells need a kind of dormancy during winter (e.g. freezing, see Hoham and Duval 2001) before they will germinate during the next season.

Acknowledgements We thank the Institute of Ecology, University of Innsbruck, for admittance to their Limnological Field Station at Lake Gossenkölle (Tyrol) and the Austrian Science Fund FWF (Project 200810 to C. L.) for support. U. K. thanks the Deutsche Forschungsgemeinschaft (KA 899/16-1) for a grant which supported his sabbatical at the University of Innsbruck. T. L. also is indebted to the Deutsche Forschungsgemeinschaft for funding his snow algal research (LE 1275/2-2). Furthermore, we thank Hans Wastian and Siegfried Aigner for assistance in the field, Werner Kofler for the SEM image generation, Belina DeCarli for TEM sectioning and image creation, Thomas Pröschold for providing the gene sequence of strain CCCryo 154-01 as well as Christian Wiencke (AWI Bremerhaven) for lending the PAM.

Conflict of interest The authors declare that they have no conflict of interest.

References

Bidigare RR, Ondrusek ME, Kennicutt MC II, Iturriaga R, Harvey HR, Hoham RW, Macko SA (1993) Evidence for a photoprotective function for secondary carotenoids of snow algae. J Phycol 29:427–434

Bischoff Y (2008) Diversité et mobilité des algues de neige dans les Alpes suisses. Dissertation, University of Geneva, p. 132

Brown RM, Johnson SC, Bold HC (1968) Electron and phase-contrast microscopy of sexual reproduction in *Chlamydomonas moewusii*. J Phycol 4:100–120

Buchner O, Lütz C, Holzinger A (2007) Design and construction of a new temperature controlled chamber for light- and confocal microscopy under monitored conditions: biological application for plant samples. J Microsc 225:183–191

Cavalier-Smith T (1976) Electron microscopy of zygospore formation in *Chlamydomonas reinhardii*. Protoplasma 87:297–315

Duval B, Shetty K, Thomas WH (2000) Phenolic compounds and antioxidant properties in the snow alga Chlamydomonas nivalis after exposure to light. J Appl Phycol 11:559–566

Ettl H (1968) Ein beitrag zur kenntnis der algenflora tirols. Ber nat-med Ver Innsbruck 56:177–354

Ettl H (1983) Chlorophyta I. Phytomonadina. In: Ettl H, Gerloff J, Heynig H, Mollenhauer D (eds) Süßwasserflora von Mitteleuropa, vol. 9. Gustav Fischer, Stuttgart, p 807

Gorton HL, William WE, Vogelmann TC (2001) The light environment and cellular optics of the snow alga *Chlamydomonas nivalis* (Bauer) Wille. Photochem Photobiol 73:611–620

Hagen C, Siegmund S, Braune W (2002) Ultrastructural and chemical changes in the cell wall of *Haematococcus pluvialis* (Volvocales, Chlorophyta) during aplanospore formation. Eur J Phycol 37:217–226

Hanagata N (1998) Phylogeny of the subfamily Scotiellocystoideae (Chlorophyceae, Chlorophyta) and related taxa inferred from 18 s ribosomal rna gene sequence data. J Phycol 34:1049–1054

Hanahan D (1983) Studies on transformation of *Escherichia coli* with plasmids. J Mol Biol 166:557–580

Hancke TB, Hancke K, Johnsen G, Sakshaug E (2008) Rate of O_2 production derived from pulse-amplitude-modulated fluorescence: testing three biooptical approaches against measured O_2 production rate. J Phycol 44:803–813

Harris EH (2009) The *Chlamydomonas* sourcebook. Volume 1: introduction to *Chlamydomonas* and its laboratory use, 2nd edn. Academic Press, Oxford, p 444

Henley WJ (1993) Measurement and interpretation of photosynthetic light-response curves in algae in the context of photoinhibition and diel changes. J Phycol 29:729–739

Hepler PK, Newcomb EH (1964) Microtubules and fibrils in the cytoplasm of *Coleus* cells undergoing secondary wall deposition. J Cell Biol 20:529–533

Hoham RW, Blinn DW (1979) Distribution of cryophilic algae in an arid region, the American Southwest. Phycologia 18:133–145

Hoham RW, Mullet JE (1977) The life history and ecology of the snow alga *Chloromonas cryophila* sp. nov. (Chlorophyta, Volvocales). Phycologia 16:53–68

Hoham RW, Mullet JE (1978) *Chloromonas nivalis* (Chod.) Hoh. & Mull. Comb. Nov., and additional comments on the snow alga, *Scotiella*. Phycologia 17:106–107

Hoham RW, Duval B (2001) Microbial ecology of snow and freshwater ice with emphasis on snow algae. In: Jones et al (eds) Snow ecology. Cambridge University Press, New York, pp 168–228

Hoham RW, Roemer SC, Mullet JE (1979) The life history and ecology of the snow alga *Chloromonas brevispina* comb. nov. (Chlorophyta, Volvocales). Phycologia 18:55–70

Hoham RW, Bonome TA, Martin CW, Leebens-Mack JH (2002) A combined 18S rDNA and *rbc*L phylogenetic analysis of *Chloromonas* and *Chlamydomonas* (Chlorophyceae, Volvocales) emphasizing snow and other cold-temperate habitats. J Phycol 38:1051–1064

Hoham RW, Berman JD, Rogers HS, Felio JH, Ryba JB, Miller PR (2006) Two new species of green snow algae from Upstate New York, *Chloromonas chenangoensis* sp. nov. and *Chloromonas tughillensis* sp. nov. (Volvocales, Chlorophyceae) and the effects of light on their life cycle development. Phycologia 45:319–330

Holzinger A, Lütz C (2006) Algae and UV irradiation: effects on ultrastructure and related metabolic functions. Micron 37:190–207

Karsten U, Friedl T, Schumann R, Hoyer K, Lembcke S (2005) Mycosporine like amino acids (MAAs) and phylogenies in green algae: *Prasiola* and its relatives from the Trebouxiophyceae (Chlorophyta). J Phycol 41:557–566

Karsten U, Escoubeyrou K, Charles F (2009) The effect of redissolution solvents and HPLC columns on the analysis of

mycosporine-like amino acids (MAAs) in the macroalgal species *Prasiola crispa* and *Porphyra umbilicalis*. Helgol Mar Res 63:231–238

Kol E (1968) Kryobiologie. Biologie und Limnologie des Schnees und Eises. I. Kryovegetation. In: Elster HJ, Ohle W (eds) Die Binnengewässer, Band XXIV. Schweizerbart'sche Verlagsbuchhandlung, Stuttgart, p 216

Kol E (1970) Vom roten Schnee der Tiroler Alpen. Ann Hist-Nat Mus Natl Hung 62:129–136

Komárek J, Nedbalová L (2007) Green cryosestic algae. In: Seckbach J (ed) Cellular origin, life in extreme habitats and astrobiology (volume 11): algae and cyanobacteria in extreme environments, part 4: phototrophs in cold environments. Springer, Dordrecht, pp 323–344

Kromkap JC, Forster RM (2003) The use of variable fluorescence measurements in aquatic ecosystems: differences between multiple and single turnover measuring protocols and suggested terminology. Eur J Phycol 38:103–112

Kvíderova J, Stibal M, Nedbalová L, Kaštovská K (2005) The first record of snow algae vitality in situ by variable fluorescence of chlorophyll. Fottea 5:69–77

Leslie GA (2009) Natural products in plants: chemical diversity. In: Begley TP (ed) Wiley Encyclopedia of Chemical Biology, vol. 3. Willey, Hoboken, N.J., pp 261–277

Leya T (2004) Feldstudien und genetische Untersuchungen zur Kryophilie der Schneealgen Nordwestspitzbergens. Dissertation. Shaker, Aachen, p 145

Leya T, Rahn A, Lütz C, Remias D (2009) Response of arctic snow and permafrost algae to high light and nitrogen stress by changes in pigment composition and applied aspects for biotechnology. FEMS Microbiol Ecol 67:432–443

Li HB, Cheng KW, Wong CC, Fan KW, Chen F, Jiang Y (2007) Evaluation of antioxidant capacity and total phenolic content of different fractions of selected microalgae. Food Chem 102:771–776

Liaaen-Jensen S, Lutnæs BJ (2008) *E/Z* isomers and isomerization. In: Britton G, Liaaen-Jensen S, Pfander H (eds) Carotenoids, volume 4: natural functions. Birkhäuser, Basel, pp 15–36

Ling HU, Seppelt RD (1998) Snow algae of the Windmill Islands, continental Antarctica. 3. *Choloromonas polyptera* (Volvocales, Chlorophyta). Polar Biol 20:320–324

Lukavský J (1993) First record of cryoseston in the Bohemian Forest Mts. (Šumava). Algological Stud 69:83–89

Lukavský J, Furnadzhieva S, Nedbalová L (2009) First record of cryoseston in the Vitosha Mountains (Bulgaria). Nova Hedwigia 88:97–109

Marshall WA, Chalmers MO (1997) Airborne dispersal of Antarctic terrestrial algae and cyanobacteria. Ecography 20:585–594

Masojidek J, Kopecký J, Kobližek M, Torzillo G (2004) The xanthophyll cycle in green algae (Chlorophyta): its role in the photosynthetic apparatus. Plant Biology 6:342–349

Müller T, Bleiß W, Martin CD, Rogaschewski S, Fuhr G (1998) Snow algae from northwest Svalbard: their identification, distribution, pigment and nutrient content. Polar Biol 20:14–32

Muramoto K, Kato S, Shitara T, Hara Y, Nozaki H (2008) Morphological and genetic variation in the cosmopolitan snow alga *Chloromonas nivalis* (Volvocales, Chlorophyta) from Japanese mountainous area. Cytologia 73:91–96

Nedbalová L, Kociánová M, Lukavský J (2008) Ecology of snow algae in the Giant Mts. Opera Corcon 45:59–68

Novis PM, Hoham RW, Beer T, Dawson M (2008) Two snow species of the quadriflagellate green alga *Chlainomonas* (Chlorophyta, Volvocales): ultrastructure and phylogenetic position within the *Chloromonas* clade. J Phycol 44:1001–1012

Posada D, Crandall KA (1998) Modeltest: testing the model of DNA substitution. Bioinformatics 14:817–818

Pröschold T, Marin B, Schlösser UG, Melkonian M (2001) Molecular phylogeny and taxonomic revision of *Chlamydomonas* (Chlorophyta). I. Emendation of *Chlamydomonas* Ehrenberg and *Chloromonas* Gobi, and description of *Oogamochlamys* gen. nov. and *Lobochlamys* gen. nov. Protist 152:265–300

Remias D, Lütz-Meindl U, Lütz C (2005) Photosynthesis, pigments and ultrastructure of the alpine snow alga Chlamydomonas nivalis. Eur J Phycol 40:259–268

Remias D, Lütz C (2007) Characterisation of esterified secondary carotenoids and of their isomers in green algae: a HPLC approach. Algological Stud 124:85–94

Remias D, Holzinger A, Lütz C (2009) Physiology, ultrastructure and habitat of the ice alga *Mesotaenium berggrenii* (Zygnemaphyceae, Chlorophyta) from glaciers in the European Alps. Phycologia 48:302–312

Řezanka T, Nedbalová L, Sigler K, Cepák V (2008) Identification of astaxanthin diglucoside diesters from snow alga *Chlamydomonas nivalis* by liquid chromatography–atmospheric pressure chemical ionization mass spectrometry. Phytochemistry 69:479–490

Schreiber U, Schliwa U, Bilger W (1986) Continuous recording of photochemical and nonphotochemical chlorophyll fluorescence quenching with a new type of modulation fluorometer. Photosynth Res 10:51–62

Stibal M (2003) Ecological and physiological characteristics of snow algae from Czech and Slovak mountains. Fottea (Czech Phycology) 3:141–152

Stibal M, Elster J, Šabacká M, Kaštovská K (2007) Seasonal and diel changes in photosynthetic activity of the snow alga *Chlamydomonas nivalis* (Chlorophyceae) from Svalbard determined by pulse amplitude modulation fluorometry. FEMS Microbiol Ecol 59:265–273

Tamura K, Nei M (1993) Estimation of the number of nucleotide substitutions in the control region of mitochondrial DNA in humans and chimpanzees. Mol Biol Evol 10:512–526

Tschaikner A, Ingolić E, Stoyneva MP, Gärtner G (2007) Autosporulation in the soil alga *Coelastrella terrestris* (*Chlorophyta*, *Scenedesmaceae*, *Scenedesmoideae*). Phytol Balc 13:29–34

Webb WL, Newton M, Starr D (1974) Carbon dioxide exchange of *Alnus rubra*: a mathematical model. Oecol 17:281–291